Received: 4 July 2023 | Revised: 20 December 2023 | Accepted: 29 December 2023

DOI: 10.1002/hyp.15084

RESEARCH ARTICLE

WILEY

Enhancing hydrological model calibration through hybrid strategies in data-scarce regions

Vicky Anand[1,2] | Bakimchandra Oinam[1] | Silke Wieprecht[2] | Shailesh Kumar Singh[3] | Raghavan Srinivasan[4]

[1]Department of Civil Engineering, National Institute of Technology Manipur, Imphal, India

[2]Department of Hydraulic Engineering and Water Resources Management, Institute for Modeling Hydraulic and Environmental Systems, University of Stuttgart, Stuttgart, Germany

[3]National Institute of Water and Atmospheric Research, Christchurch, New Zealand

[4]Department of Ecology and Conservation Biology, Texas A&M University, College Station, Texas, USA

Correspondence
Vicky Anand, Department of Hydraulic Engineering and Water Resources Management, Institute for Modeling Hydraulic and Environmental Systems, University of Stuttgart, Stuttgart, Germany
Email: vicky.einstein@gmail.com

Funding information
SERB, Grant/Award Number: CRG/2021/006665; The Ministry of Education, Govt. of India; Deutscher Akademischer Austauschdienst; National Institute of Technology Manipur

Abstract

Calibration of a hydrological model is a challenging task, especially in basins that are data scarce. With the incorporation of regional information and integration with satellite data, the parameters of hydrological models can be estimated for a basin with scant or no discharge records. The main objective of this study is to calibrate and validate a hydrological model based on a limited amount of in-situ measured and remote sensing satellite datasets in a data-sparse region. Multiple techniques were applied for the model calibration: (1) stage-discharge curves using a spatial proximity approach, (2) Simplified Surface Energy Balance actual evapotranspiration, (3) river discharge using a physical similarity regionalization approach, and (4) a new hybrid approach by integrating remote sensing datasets along with field measured river bathymetry data to estimate the river discharge. To demonstrate the methodology, we employed the widely used Soil and Water Assessment Tool (SWAT) hydrological model in Manipur River Basin, India. The sensitivity, calibration, and validation of the SWAT model were carried out by using the Sequential Uncertainty Fitting Technique. During calibration, the coefficient of determination (R^2) and the Kling Gupta Efficiency (KGE) were found to be in the range of 0.46–0.81 and 0.41–0.83, whereas during validation R^2 and KGE were found to be in the range of 0.40–0.79 and 0.53–0.77 for the four different techniques. Among all the four techniques applied in this study, calibration based on (i) stage-discharge curve using spatial proximity approach and (ii) new hybrid approach by integrating remote sensing datasets and river bathymetry were found as the better approaches as indicated by the statistical indices. The performance evaluation of the model through a new hybrid approach by integrating remote sensing and in-situ measured datasets for rivers with narrow width represents a promising technique for use in a data sparse region.

KEYWORDS
bathymetry, evapotranspiration, Kling Gupta efficiency, regionalization, sequential uncertainty fitting technique, soil and water assessment tool

1 | INTRODUCTION

Hydrological models facilitate the user in understanding the interaction between the several parameters of the complex hydrological system and assist the user in predicting the spatio-temporal information of the basin (Pechlivanidis et al., 2011; Sokolowski & Banks, 2010). Hydrological models serve as an interface between theory and practice by simplifying the hydrological system that depicts hydrological processes. This allows users to analyse phenomena at basin, regional, and global scales that are in synchronous with the hydrological systems. (Babel & Karssenberg, 2013; Singh et al., 2020; Tessema, 2011). Hydrological modelling is a useful tool for various purposes such as water resources planning and management but it is always a challenging task to carry out hydrological modelling in a data-scarce region due to the deficit in quantity and quality of data. In general, in-situ measurement of all the data associated with hydrological processes and systems is not feasible at basin or sub-basin scale. The field measurements have limitations as they are time-consuming, cost-heavy and have constraints due to the systems' higher temporal and spatial heterogeneity.

Hydrological systems have nonlinear complex dynamics that are difficult to comprehend. (Sokolowski & Banks, 2010). Calibration and validation are a vital part of the hydrological modelling on a basin scale due to the higher spatio-temporal variability in the hydrological system. Calibration and validation of model depends upon the availability and the resolution of the observed datasets. In a gauged basin with the availability of observed discharge data of a river, the moisture and nitrogen content in the soil as well as evapotranspiration can be modelled with good accuracies (Odusanya et al., 2019). However, hydrological modelling is a complex task in a scantly gauged region or basin due to distinct features of the hydro-climatological parameters especially in the tropical and semi-tropical regions (Ajami et al., 2004; Bardossy, 2007; Singh & Bárdossy, 2015; Thomas et al., 2013). Several investigations have been undertaken by applying the Soil and Water Assessment Tool (SWAT) hydrological model in different basins in data-scarce locations (Emam et al., 2017; Liu et al., 2015; Mengistu et al., 2019; Qi et al., 2020; Sirisena et al., 2020; Swain & Patra, 2017); the key drawback of these researches was the spatiotemporal coverage of the data used for calibration and validation. Although all of these earlier studies on SWAT applications attempted to enhance model performance in catchments with less data, they did find some variation in model performance.

River discharges are measured at gauging stations. Even yet, recorded statistics are unreliable, particularly in developing and underdeveloped countries, and are subject to proprietary control in developed countries (Tarpanelli et al., 2013). These defy the bounds of the research studies related to hydrological modelling which requires river discharge datasets. In the past decades satellite remote sensing datasets have provided an aid in a data scarce region (Ali et al., 2023). Remote sensing-based data or product offers extensive coverage of water bodies like rivers, lakes and ponds. In the recent past, several research studies have indicated the advantages of remote sensing in terms of its extensive monitoring period and spatial coverage. Both edges have increased attention in deriving streamflow approximation from remote sensing (Huang et al., 2020; Sichangi et al., 2016). However, remote sensing datasets have their own limitation while estimating the discharge of medium to small size stream due to its spatial resolutions (Anand et al., 2023; Lou et al., 2022).

There are several hydrologic models (e.g., empirical models, lumped models, statistical models, physically distributed models) to compute the availability of water resources. Physically distributed models aim to illustrate the hydrologic processes in details and can predict the quality and quantity of water with respect to both time and space (Odusanya et al., 2019). These predictions are based on several parameters such as climatic condition, soil, land use land cover, and topography of the region. There are numerous physical-based models, such as SHETRAN, which can model sub-surface flow and transport (Ewen et al., 2000), the Hydrologic Simulation Program Fortran which can model the nutrient flow in streams (Bicknell et al., 1997), variable infiltration capacity which can model the energy and water balances at the macroscopic scale (Liang et al., 1994), and SWAT which can model and predict the water quality and quantity and represents land management practices (Arnold et al., 1998). According to Odusanya et al. (2019), these physical-based models may clearly illustrate the physical, biological, and chemical processes in the basin by means of their underlying physical mechanisms.

In this study, the widely used Soil and Water Assessment Tool (SWAT) hydrological model was employed in the Manipur River Basin, India, to demonstrate the methodology using multiple techniques based on both in-situ measured and remote sensing satellite datasets. Several studies have been done to estimate the discharge of an ungauged river basin solely with remote sensing datasets which can be used for model calibration but they have been limited to rivers with large width (Kebede et al., 2020; Xueying et al., 2023). In the past, Getirana (2010) used Envisat-derived water levels with empirical formulas in Amazon River basin, Sun et al. (2012) used TOPEX derived water levels with AHG, Paris et al. (2016) used Jason-2 and Envisat derived water levels with rating curves in the Amazon River basin, Huang et al. (2020) used Jason-2-derived water levels and Surface Water and Ocean Topography (SWOT)-like data with developed empirical equations in Upper Brahmaputra River, to derive river discharge. This study presents a new hybrid approach by integrating remote sensing datasets along with field measured river bathymetry data to estimate the river discharge to calibrate the SWAT hydrological model in a river with narrow width.

The main objective of this study is to calibrate and validate the SWAT hydrological model based on a limited amount of in-situ measured and remote sensing satellite datasets. Multiple techniques were applied based on (1) Stage-discharge curves using spatial proximity approach, (2) Simplified Surface Energy Balance (SSEBop) actual evapotranspiration derived from MODIS, (3) river discharge using a physical similarity regionalization approach, and (4) hybrid approach by integrating remote sensing, water level and river bathymetry.

2 | MATERIALS AND METHODS

2.1 | Study area

To demonstrate the methodology, we selected the Manipur River basin located in North-Eastern part of India. The Manipur River basin,

along with the Barak River basin and Yu River basin, drains the North-Eastern state of Manipur. The Manipur River basin is the largest river basin in the valley region of Manipur and covers 28% of the state's total area (Singh et al., 2010). The major section of the Manipur River basin comprises the valley region of Manipur and plays a critical role in the socio-economic condition of the region (Anand et al., 2020). In the past few decades, there has been a significant change in eco-hydraulic and eco-hydrologic conditions in the basin due to natural and anthropogenic factors. Observed hydrometric data (such as streamflow) and its quality in terms of its consistency are missing in the basin as it is ungauged. The longitudinal and latitudinal extent of the Manipur River basin is between 24° and 25°25′ North and 93°36′–94°27′ East. The Manipur River basin is hydrologically divided into nine sub-basins, namely Sekmai, Thoubal, Nambol, Imphal, Heirok, Kongba, Western, Iril and Khuga. Iril and Thobal rivers are the largest tributaries of the Manipur River. Loktak Lake, one of the distinctive ecological units in Manipur, is one of the vital sub-basins of the Manipur River basin (LDA, 2003; Ramsar Bureau, 2016). The Loktak Lake is located in the central valley and covers 28% of the total area of the Manipur River basin (Singh et al., 2011). The unique element of the lake is the *"Phumdis"*, herbaceous floating biomass (LDA, 2003). The Keibul Lamjao National Park, the only floating national park in the world located on the south-eastern side of the Loktak Lake, is the only natural habitat of *Rucervus Eldii* (LDA, 2003). The total area of the basin is 5020 km^2. The elevation varies from 744 to 2689 m above MSL with mild slope in the valley region to steep slope in the hilly region. The study area is shown in Figure 1.

The Manipur river basin is characterized by a semi-tropical to a tropical type of climate. In contrast, the hilly regions in the northern part of the basin experience temperate to a semi-temperate type of climate (Directorate of Environment, 2013). India's southwest monsoon winds drive the climate in this basin. The basin receives an

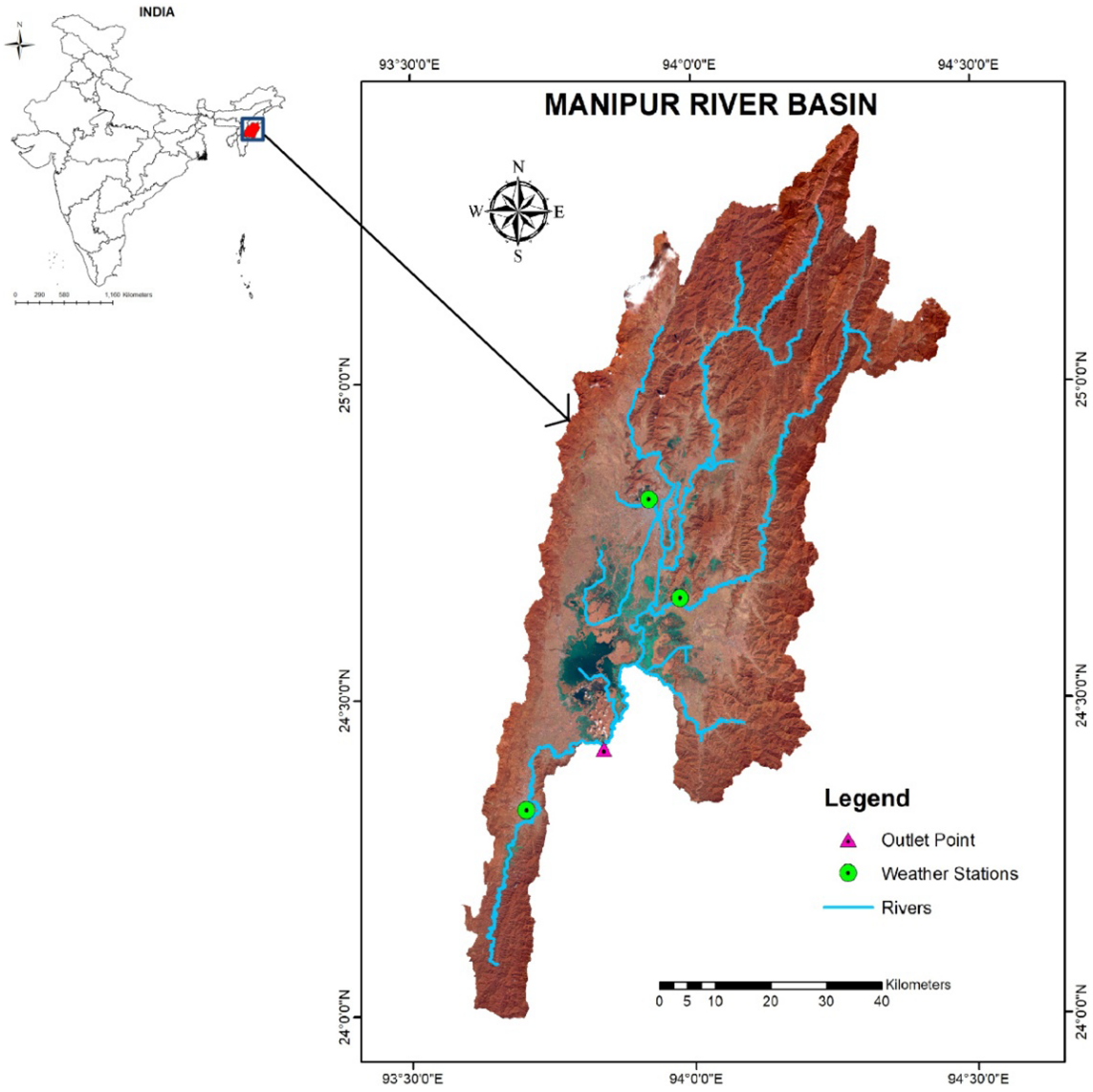

FIGURE 1 Manipur river basin with the meteorological stations, outlet point and river network.

annual average rainfall of 1350 mm (Directorate of Environment, 2013). The monsoon season starts from mid-June, lasts till mid-October, and accounts for 63% of the annual rainfall in the basin (Directorate of Environment, 2013). The relative humidity ranges in the basin between 51% and 81%, and the mean annual temperature ranges from 12 to 31°C, with May as the hottest and January as the coldest month, respectively. The basin is mostly dominated by forest and agriculture. Forest cover mainly consists of moist deciduous and subtropical pine forests. Rock types are mostly igneous intrusions and Cretaceous and Tertiary sedimentary formations (NBSS and LUP, 2001). The major soils of the basin are Haplohumults, Dystrocrepts, Hapludalfs, and Haplaquepts (NBSS and LUP, 2001).

2.2 | Data acquisition and analysis

The SWAT model was set-up for the Manipur River basin using Land Use Land Cover (LULC) data, a Digital Elevation Model (DEM), meteorological data and soil data as input variables. The ALOS PALSAR DEM was used in this study to delineate the watershed. The LULC for the study area was generated based on Landsat 8 OLI C1 Level 1 image using maximum likelihood classifiers for the year 2017. The soil data were obtained from the National Bureau of Soil Survey and Land Use Planning (NBSS and LUP), Govt. of India. Meteorological data from three different gauging stations were obtained on a daily time scale. Due to the lack of hydrometric stations in the basin, direct streamflow was unavailable for the model calibration. In order to calibrate the model, various approaches were adopted using the datasets obtained from multiple organizations. A detailed description of the adopted approaches has been discussed in the Section 2.8. The details of the datasets, along with their source and resolution, are shown in Table 1.

TABLE 1 Input dataset with its source and resolution.

Data	Resolution	Source
Digital Elevation Model (DEM)	12.5 m	ALOS PALSAR, Alaska Satellite Facility
Land use Land cover[a]	30 m	Landsat 8, Earth resource observation and science
Meteorological data	Daily	Directorate of Environment Manipur
Soil data[a]	1:500000	National Bureau of Soil Survey & Land Use Planning (NBSS & LUP)
Manipur river water level	Monthly	National Hydro Electric Power Corporation (NHPC) Power Station Loktak Project (January 2008–December 2018)
Manipur river water level and discharge	Daily	Loktak Development Authority (April 2000–March 2002)
Multispectral data	5.8 m	LISS-IV, Resourcesat 2A, National Remote Sensing Centre (NRSC), Indian Space Research Organization (ISRO)
Manipur River cross-section	1 m	Field survey using echo-sounder
Evapotranspiration	Monthly	SSEBop (2004–2018)
Dhansiri River discharge	Monthly	Inland Waterways Authority of India (IWAI) (2016)

[a]Resampled to 12.5 m.

2.3 | SWAT hydrological model

SWAT is an open-source physical-based semi-distributed ecohydrological model (Arnold et al., 1998). SWAT works on a three-phase system in which the basin is divided into sub-basins and sub-basins into their smallest units, known as hydrological response units (HRUs) (Arnold & Fohrer, 2005). Using various methods, the model can compute nutrient, water, and sediment flow within a watershed (Arnold & Fohrer, 2005). In SWAT, the land phase equation governs the hydrological cycle. A detailed description of SWAT is given in the manual (Neitsch et al., 2002). SWAT is based on the water balance equation (Equation 1) (Arnold & Fohrer, 2005).

$$SW_t = SW_o + \sum_{j=0}^{n} \left(P_{day} - Q_{sur} - E_a - W_{sep} - Q_{gw}\right), \quad (1)$$

where SW_t is the quantity of water content in the soil after t days (mm); SW_0 is the initial quantity of water content in the soil on j^{th} day (mm); P_{day} is the quantity of precipitation on j^{th} day (mm); Q_{gw} is the quantity of return flow on j^{th} day; E_a is the quantity of evapotranspiration on j^{th} day (mm); Q_{sur} is the quantity of surface runoff on j^{th} day (mm); W_{sep} is the quantity of percolation going into the vadose zone on j^{th} day, and t is the amount of time in days.

Sensitivity analysis and calibration were carried out in the Soil and Water Assessment Tool-Calibration and Uncertainty Programming (SWAT-CUP). Sampling methods applied to carryout sensitivity analysis were one-factor-at-a-time (OAT) and Latin hypercube (Abbaspour, 2015). There are several algorithms embedded in SWAT-CUP to carryout calibration: Sequential Uncertainty Fitting Technique (SUFI-2), Markov Chain Monte Carlo, Generalized Likelihood Uncertainty Estimation, particle swarm optimization and Parameter Solution (Abbaspour, 2015). In this study, SUFI-2 was applied to carryout calibration and validation of the model as SUFI-2 is the only algorithm in SWAT-CUP which is global.

2.4 | Routing method in SWAT

For the calculation of concentration-time in the watershed Manning's equation is applied (Neitsch et al., 2011). In SWAT, two options are available for routing that is, the variable storage routing method and the Muskingum routing method (Neitsch et al., 2011). In order to compute all the essential geometric parameters of the channel, SWAT uses channel's depth at the top of the bank (dbankfull), the width of water up to bankfull depth (Wbankfull), Manning's coefficient (n),

longitudinal channel's slope (chslp) and main channel's length (len) as an input in .rte file (Neitsch et al., 2011). For the purpose of flood routing, SWAT assumes the cross-section of the channel to be trapezoidal, with the side slope of the flood plain as 1:2 and the main channel as 1:4. In this study, the Muskingum routing method embedded in SWAT was applied. Conceptually the Muskingum routing method used in SWAT is derived from the Muskingum Cunge method (Cunge, 1969), which uses the matched diffusivity concept. The routing equation is (Equations 2–9):

$$Out_2 = C_1 In_2 + C_2 In_1 + C_3 Out_1, \tag{2}$$

where

$$C_1 = \frac{-2K\theta + \Delta t}{2K(1-\theta) + \Delta t}, \tag{3}$$

$$C_2 = \frac{2K\theta + \Delta t}{2K(1-\theta) + \Delta t}, \tag{4}$$

$$C_3 = \frac{2K(1-\theta) - \Delta t}{2K(1-\theta) + \Delta t}, \tag{5}$$

where K is storage constant for reach (s), In_2 is final inflow (m^3s^{-1}), In_1 is initial inflow (m^3s^{-1}), Out_2 is final outflow (m^3s^{-1}), Out_1 is initial outflow (m^3s^{-1}), θ = *weighting factor*.

The following clause is recommended in SWAT to avoid a negative outflow calculation and ensure numerical stability.

$$2K\theta < \Delta t < 2K(1-\theta), \tag{6}$$

$$K = a_1 K_{bankfull} + a_2 K_{0.1bankfull}, \tag{7}$$

where a_1 and a_2 are weighted quantities defined by the user. The value of $K_{bankfull}$ and $K_{0.1bankfull}$ is computed using the formula given by (Cunge, 1969). K is storage constant, defined as routing step length divided by the wave celerity.

$$K = \frac{1000 L_k}{C_k}, \tag{8}$$

where L_k is the length of the channel and C_k is the celerity of the flood wave

$$C_k = \frac{\partial Q}{\partial A} = \frac{5}{3} v_c, \tag{9}$$

where v_c is the flow velocity in the channel.

2.5 | Evapotranspiration in SWAT

Evapotranspiration plays a vital role in water balance. There are several methods to estimate Potential Evapotranspiration (PET), but it is complex to determine the Actual Evapotranspiration (AET). It is often deduced from the PET through a cause that demonstrates the intensity of stress experienced by plants. In SWAT, there are three options to compute PET: the Hargreaves method, the Priestley-Taylor method, and the Penman-Monteith method. In this study, the Penman-Monteith method was adopted. Wind speed, air temperature, relative humidity, and solar radiation are required as input in the Penman-Monteith method (Equation 10).

$$\lambda E = \frac{\Delta \times (H_{net} - G) + \rho_{air} \times C_p \times (e_z^o - e_z)/r_a}{\Delta + \gamma \times (1 + r_c/r_a)}, \tag{10}$$

where λE denotes latent heat flux density (MJ $m^{-2}d^{-1}$), H_{net} denotes net radiation (MJ $m^{-2}d^{-1}$), Δ denotes slope of saturation vapour pressure–temperature curve (kPa $^\circ C^{-1}$), ρ_{air} denotes air density (kg m^{-3}), E denotes the depth rate evaporation (mm d^{-1}), C_p denotes specific heat at constant pressure (MJ kg^{-1} $^\circ C^{-1}$), G denotes heat flux density to the ground (MJ $m^{-2}d^{-1}$), γ denotes psychrometric constant (kPa $^\circ C^{-1}$), r_a denotes aerodynamic resistance (s m^{-1}), r_c denotes plants canopy resistance, e_z denotes water vapour pressure of air at height z (kPa), and e_z^o denotes saturation vapour pressure at height z (kPa).

2.6 | Estimation of discharge and Manning's roughness coefficient based on remote sensing datasets

Estimating the discharge of rivers is complex; therefore, they are calculated based on hydraulic parameters derived from the field-based survey or remotely sensed datasets using mathematical equations. Using Manning's fundamental open channel flow, the channel (river) discharge can be computed as (Manning, 1891) (Equation 11).

$$Q = \frac{1}{n} \times A \times R^{2/3} \times S^{1/2}, \tag{11}$$

where S is the friction slope, R is the hydraulic radius, A is the wetted area and n is the Manning's roughness coefficient.

Channel irregularity, vegetation cover, degree of meandering of the stream, the consequence of obstruction, and the materials involved are the various parameters influencing the channel's resistance (Coon, 1998). Numerous methods have been already proposed to estimate channel's resistance: assigning a proper value from Table 2 (Chow, 1959), by visual interpretation and ground survey (Dudley et al., 1998). In this study, Resourcesat 2A LISS IV with a 5.8 m high spatial resolution satellite imagery was implemented along with the colour composite approach with visual interpretation to estimate the channel's resistance at the outlet. The channel roughness coefficient was estimated through visual image interpretation of multi-spectral satellite imagery using the formula (Equation 12)

$$n = (n_o + n_1 + n_2 + n_3 + n_4) \times n_5. \tag{12}$$

Since Manning equation is an empirical equation, the values for Manning constant are derived from observations. The equation is practically tested; are best suited for uniform, steady-state open

TABLE 2 Reference values to estimate the coefficient of roughness (Chow, 1959).

Channel condition	Sub-class		Values
Material involved	Earth	n_o	0.025
	Rock		0.025
	Fine gravel		0.024
	Course gravel		0.027
Degree of irregularity	Smooth	n_1	0.000
	Minor		0.005
	Moderate		0.010
	Severe		0.020
Variation of channel cross-section	Gradual	n_2	0.000
	Alternating occasionally		0.005
	Alternating frequently		0.010–0.015
Relative effect of obstructions	Negligible	n_3	0.000
	Minor		0.010–0.015
	Appreciable		0.020–0.030
	Severe		0.040–0.060
Vegetation	Low	n_4	0.005–0.010
	Medium		0.010–0.025
	High		0.025–0.050
	Very high		0.050–0.100
Degree of meandering	Minor	n_5	1.000
	Appreciable		1.150
	Severe		1.300

channel flow. The comprehensive methodology to estimate the coefficient of roughness of a channel from multi-spectral satellite imagery can be found in the literature by Sichangi et al. (2018) which is adapted from the methodology given by Chow (1959).

2.7 | Statistical indices for model performance and uncertainty

The coefficient of determination (R^2) (Equations 13 and 14) and Kling-Gupta efficiency (Gupta et al., 2009) (Equations 15–17) were used to evaluate the SWAT model performance during the calibration and validation (Abbaspour, 2015). In the process of evaluating the uncertainty of the model, we applied two indictors including P-factor and R-factor (Wu & Chen, 2015).

i. Coefficient of determination (R^2):

$$R^2 = \frac{\left[\sum_i \left(P_{n,i} - \overline{P_m}\right)\left(P_{t,i} - \overline{P_t}\right)\right]^2}{\sum_i \left(P_{n,i} - \overline{P_n}\right)^2 \sum_i \left(P_{t,i} - \overline{P_t}\right)^2}. \quad (13)$$

$$g = \sum_j w_j R_j^2. \quad (14)$$

ii. Kling-Gupta efficiency (KGE):

$$KGE = 1 - \sqrt{\left((r-1)^2 + (\alpha-1)^2 + (\beta-1)^2\right)}, \quad (15)$$

$$\beta = \frac{\mu_s}{\mu_m}, \alpha = \frac{\sigma_s}{\sigma_m}, \quad (16)$$

$$g = \sum_j w_j KGE_j, \quad (17)$$

where n denotes observed data, P denotes a variable, t denotes simulated data and bar signifies mean values, i denotes the i^{th} measured or simulated data, r denotes the coefficient of linear regression between simulated and observed variables, μ_s denotes the mean of simulated records, μ_m denotes the mean of observed records, σ_s denotes the standard deviation (SD) of simulated records and σ_m denotes SD of the observed data, w_j is the weight of the j^{th} variable, and g is the objective function for more than one variable.

The R-factor and the P-factor are the two indices which represent the degree of uncertainty associated with the hydrological model. The R-factor is the ratio of the average thickness of the 95% prediction uncertainty (PPU) to the standard deviation of the observed data. In contrast, the P-factor shows the percent of observed data bracketed by the 95% prediction uncertainty.

2.8 | Calibration approaches

The SWAT hydrological model was setup for Manipur river basin using DEM, landuse and soil data. After setting up the model following four approaches was adopted to calibrate the model and performance was compared.

1. Calibration based on stage-discharge curves using spatial proximity approach

Due to the lack of direct streamflow data in the basin, rating curves were generated based on the stage-discharge data collected during the hydrographic survey carried out by the Loktak Development Authority (LDA) at Arong, which is approximately 6 kilometres upstream from the outlet point. The stage-discharge data collected from the LDA was gauged three times a day at an interval of 4 h between 2000 and 2002. Based on stage-discharge data, initially, an attempt was made to generate a single rating curve for the entire season, but due to the poor performance and higher variability in discharge during the dry and wet seasons, two separate rating curves were generated for the dry and the wet season. The rating curves were generated using power regression. Later the observed discharge at the outlet point was generated using the regionalization method (i.e., spatial proximity approach) based on the stage data obtained from the National Hydroelectric Power Corporation (NHPC) Power Station Loktak Project and the generated rating curve at Arong, which is six kilometres upstream of the outlet point.

2. Calibration based on SSEBop actual evapotranspiration derived from MODIS

Several attempts have been made to calibrate the hydrological model based on the satellite remote sensing evapotranspiration datasets. Bennour et al. (2022) have used Global Land Evaporation Amsterdam Model (GLEAM) and Water Productivity Open Access Portal, whereas, Immerzeel and Droogers (2008) and Emam et al. (2017) have used moderate resolution imaging spectroradiometer (MODIS) remote sensing evapotranspiration datasets to calibrate the hydrological model. In this study, the simulated evapotranspiration of SWAT hydrological model was compared with the SSEBop actual evapotranspiration data derived from MODIS on monthly time step. The model performance was evaluated based on Kling-Gupta efficiency (KGE) and coefficient of determination. The evapotranspiration datasets were downloaded from the portal and it was mosaic. The evapotranspiration was extracted from SSEBop evapotranspiration datasets in ArcGIS and later it was summarized at sub-basin scale using zonal statistics tool. The extracted evapotranspiration was used to calibrate the SWAT hydrological model.

3. Calibration based on river discharge using physical similarity regionalization approach

In ungauged basins the hydrological parameters can be predicted through regionalization approach (e.g., Bardossy, 2007; Emam et al., 2017). Generally, the basins with similar physical characteristics shows similar hydrological responses, hence the parameters can be optimized and transferred from similar watersheds, this transformation is known as regionalization. There are several kinds of approaches for such transformation which includes spatial proximity (Emam et al., 2017), physical similarity (Mengistu et al., 2019) and regression methods (Bastola et al., 2008). Several other approaches have also been used such as ratio method to predict discharge in an ungauged basin, use of satellite altimetry data, multispectral satellite imagery-based river flow width as a substitute for river records.

In this study, Dhansiri River discharge data was used as a surrogate to ungauged Manipur River. Based on the physical similarity the area ratio method was applied as a compensation factor to the discharge of Dhansiri River in order to calibrate the hydrological model for Manipur River. The model performance and uncertainty were evaluated based on R-factor and P-factor. A high P-factor and a low R-factor quantify the minimum uncertainty associated with the model (Abbaspour et al., 2004). Nevertheless, equilibrium should be attained between the R-factor and P-factor.

4. Calibration based on water level and river bathymetry

The observed discharge of the Manipur River was computed at the outlet point using water level data obtained from the NHPC Power Station Loktak Project and the cross-sectional profile of the river. The cross-sectional profile of the river was mapped using an echo-sounder-based bathymetric survey. The actual cross-sectional profile of the river bed is shown in Figure 2a. In order to generate a regular geometric profile, multiple linear regressions were applied for the right bank, left bank and the central section of the river (Figure 2), later the channel geometry was generated and computed in AUTOCAD environment (Figure 2b). The observed discharge was generated based on the river depth and the cross-sectional profile by using Manning's equation. The coefficient of roughness was computed based on the high resolution multi-spectral satellite imageries.

3 | RESULTS

Manipur River basin is an ungauged basin, so there is a severe scarcity of data and its reliability. In order to calibrate the SWAT hydrological model in the Manipur River basin four independent techniques; based on: the stage-discharge method, regionalization of river discharge, remotely sensed actual evapotranspiration data (AET), river bathymetry, and Manning's approach were applied.

3.1 | Calibration based on stage-discharge curves using spatial proximity approach

The coefficient of determination (R^2) values of the generated stage-discharge curves was found to be 0.793 and 0.918 during the wet and the dry seasons, respectively. The coefficient of determination was found to be higher in the dry season compared to that of the wet

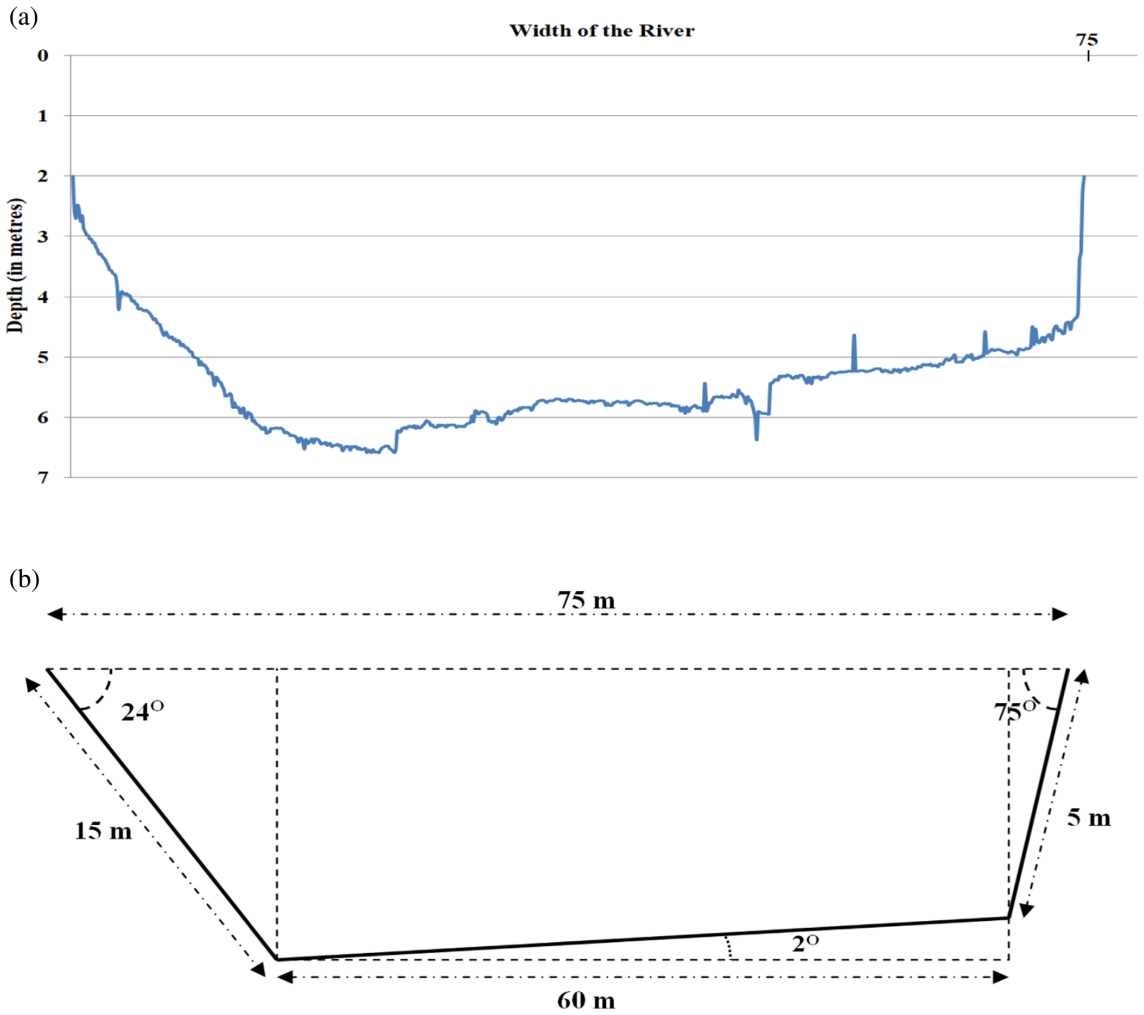

FIGURE 2 (a) Actual cross-sectional profile of the river. (b) Approximated geometric cross-sectional profile of the river.

season, mainly due to the fewer fluctuations of the flow in the dry season. In the north-eastern part of India, nestled in the Himalayan ranges, the rate of fluctuations in precipitation is very high due to the higher turbulence of the wind caused by the altitude of the Himalayan mountain ranges, which simultaneously leads to the high fluctuations in the streamflow in the rivers. The rating curve for the two different seasons is shown in Figure 3.

Model calibration was carried out between the years 2009–2015, and the validation was carried out between the years 2016–2018 on a monthly time scale, whereas the year 2008 was used as the warm-up period for the model. The sensitive variables were selected through sensitivity analysis based on the OAT technique. Then, by global sensitivity analysis, the sensitiveness of indices was found and classified as low, medium and high (Table 4). Global sensitivity shows that the initial SCS runoff curve number for moisture condition II (CN2), baseflow alpha-factor (Alpha_BF), and soil water capacity of the first soil layer (SOL_AWC) are the most sensitive parameters while calibrating the model using streamflow data obtained from the rating curve. Studies carried out in the different parts of the world also strengthen the significance of these parameters (Emam et al., 2017; Vilaysane et al., 2015). Sensitive parameters along with their fitting values are shown in (Table 4). Good agreement was detected between the simulated and observed streamflow at monthly time steps with $R^2 = 0.81$, KGE = 0.77 during the calibration and $R^2 = 0.73$, KGE = 0.70 during the validation period. Due to the spatial proximity approach, the peak value was not simulated well during the monsoon season. It can also be noted that the model performance was found to be better during calibration than validation because there was a higher uncertainty involved in the year 2017 due to the higher amount of precipitation. The calibration and validation results can be seen in Figure 4. R-factor was found to be on the lower side, with its value around 0.1 indicating the lower model uncertainty, but the P-factor value ranging around 0.5 indicates the errors are marginally not bracketed by the 95 PPU. Overall indices signify the model can be used for further eco-hydrological studies.

3.2 | Calibration based on SSEBop actual evapotranspiration derived from MODIS

The selection of SSEBop evapotranspiration products derived from MODIS was based on free availability, spatiotemporal coverage, and

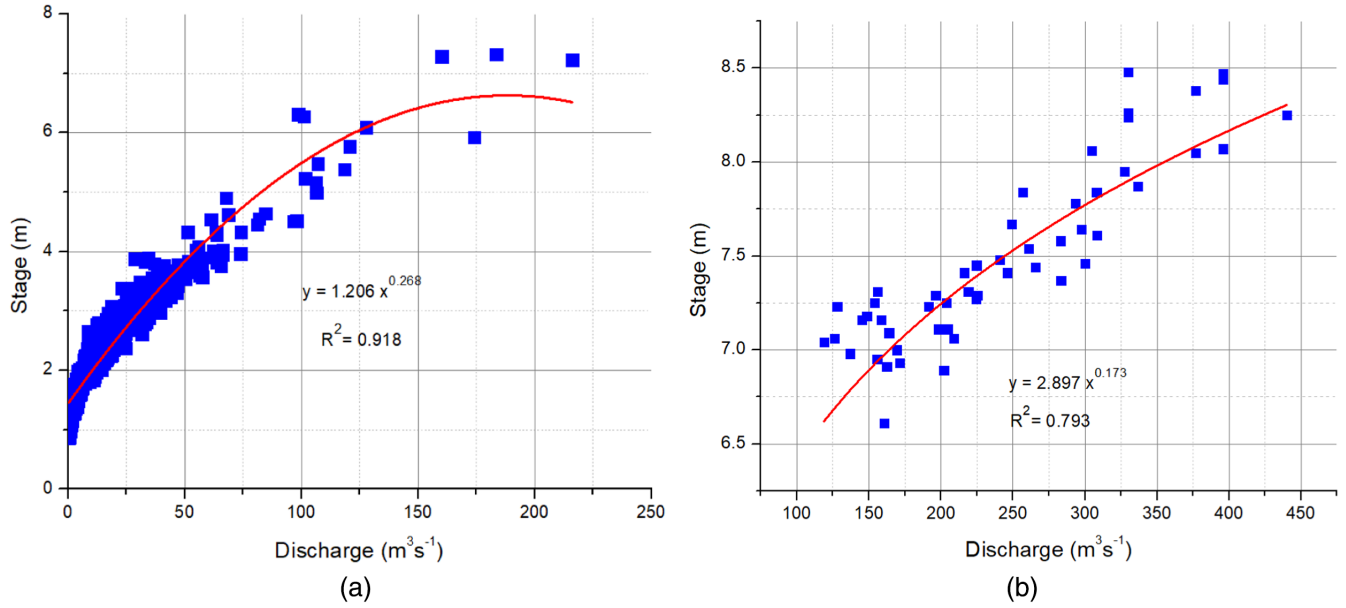

FIGURE 3 (a) Rating curve for the dry season. (b) Rating curve for the wet season.

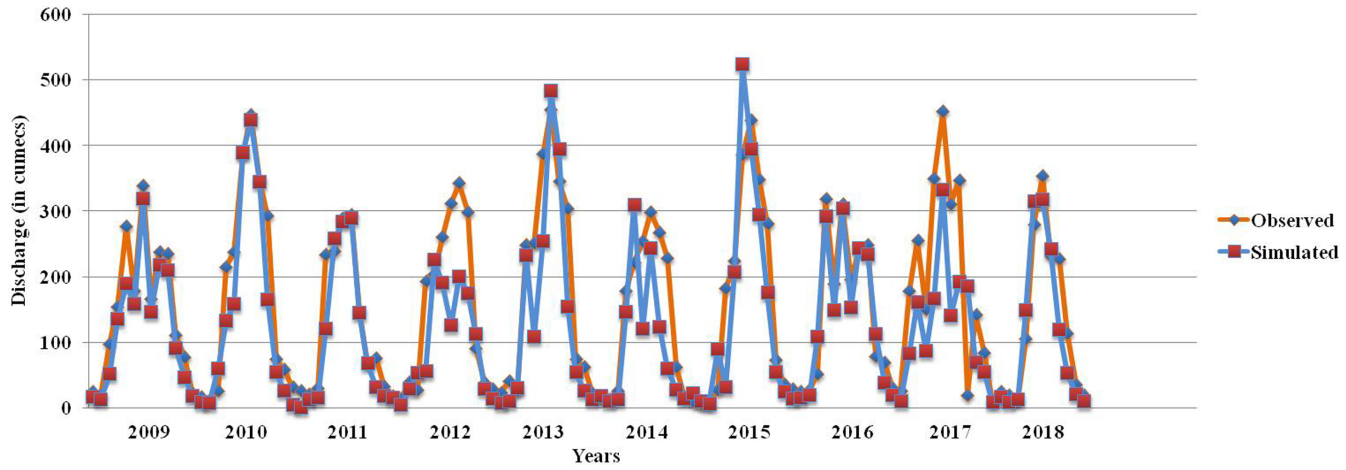

FIGURE 4 Calibration (2009–2015) and validation (2016–2018) of the model using stage-discharge curve.

resolution. SSEBop has been validated globally using data from ground observation sites (Senay et al., 2013). In the study carried out by Chen et al. (2016) found that, the uncertainties from input variables and parameters of the SSEBop model led to monthly ET estimates with relative errors less than 20%. This uncertainty of the SSEBop model lies within the error range of other surface energy balance (SEB) models, suggesting systematic error or bias of the SSEBop model is within the normal range. In this study, the SWAT hydrological model was spatially calibrated and validated at the sub-basin scale. The sub-basins located in the northern, eastern and one sub-basin in the southern part of the basin is dominated by forest. Among those, the sub-basin in the southern part was selected to optimize the relevant parameters since it is covered with dense evergreen forest. Prior to the calibration and validation of the model, parameter sensitiveness was determined based on the OAT method. In the sensitivity analysis, firstly, the sensitive variables identified in the rating-curve approach were kept the same and parameters related to the evapotranspiration phenomenon were added, that is, initial SCS runoff curve number for moisture condition II (CN2), soil evaporation compensation factor (ESCO), plant uptake compensation factor (EPCO) and maximum canopy storage (CANMAX). The vertical circulation of plant water uptake within the rooting zone is governed by the plant uptake compensation factor (EPCO), whereas soil evaporation is controlled by the soil evaporation compensation factor (ESCO), which is governed by soil characteristics. To meet the evaporative demand, more water is extracted from the lower levels as the ESCO value decreases. The quantity of water which can be trapped in a fully developed canopy and which affects the evapotranspiration, runoff, and infiltration is demonstrated by the maximum canopy storage (CANMAX).

The model was calibrated between the years 2006–2014 and validated between 2015 and 2018, whereas the time interval 2004–2005 was used as a warm-up period. During the calibration and validation period the model returned a good degree of agreement with $R^2 = 0.67$, KGE = 0.41 and $R^2 = 0.79$, KGE = 0.53 respectively. The scatter plot graph for the calibration and validation is shown in Figure 5.

From the model performance, it was observed that the actual evapotranspiration predicted by the SWAT model in the post-monsoon season was lower than the SSEBop data, but the temporal variability was predicted well by the model (Figure 6). The key parameters which play a vital role in the actual evapotranspiration variability are wind speed and relative humidity (Petković et al., 2015). During the winter months after the monsoon season, from November to February, the evapotranspiration was low due to the lower average temperature and precipitation. The model performance was found to be satisfactory based on the coefficient of determination (R^2) and KGE.

3.3 | Calibration based on river discharge using physical similarity regionalization approach

An attempt was made to calibrate the SWAT hydrological model for Manipur River using stream flow data of the Dhansiri River. This study

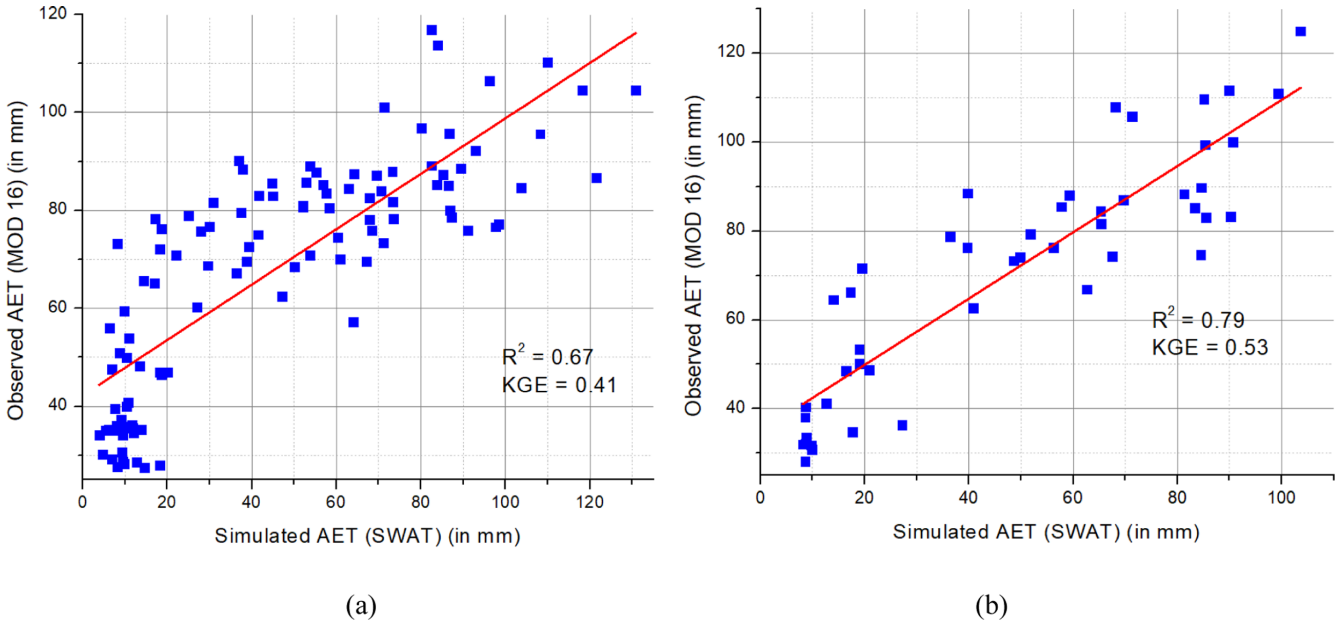

FIGURE 5 (a) Calibration. (b) Validation of model based on SSEBop AET derived from MODIS (MOD 16).

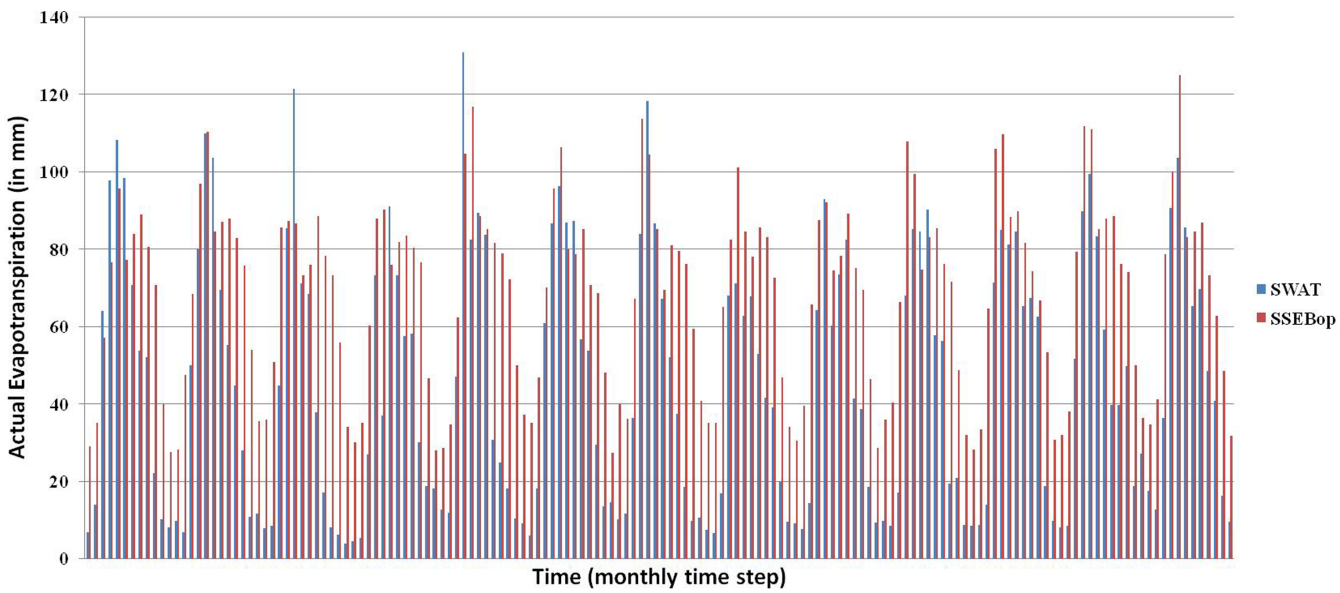

FIGURE 6 Actual evapotranspiration SWAT versus SSEBop.

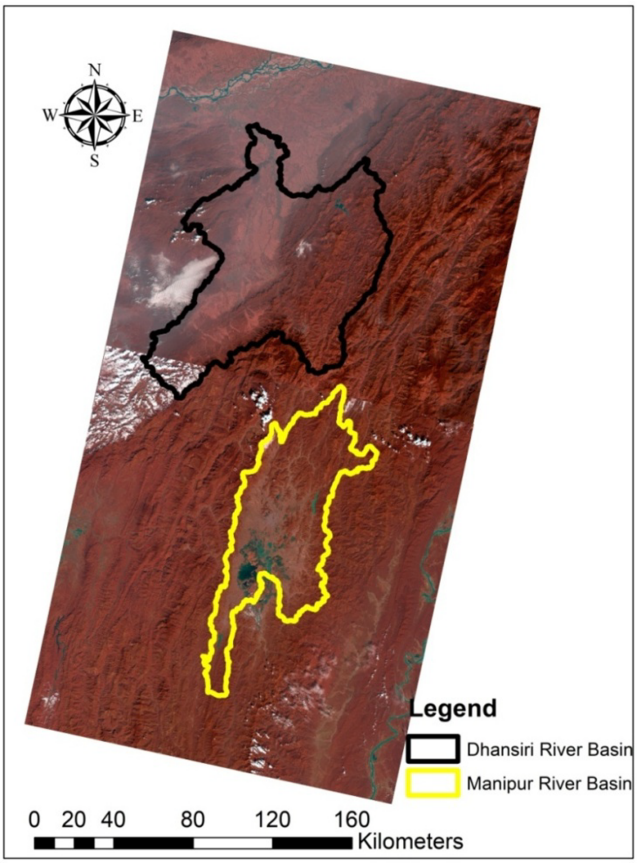

FIGURE 7 Location of the recipient basin (Manipur river basin) and the donor basin (Dhansiri river basin) showing the land features in the false colour composite (FCC).

used an observed river discharge dataset obtained from the Inland Waterways Authority of India (IWAI) (IWAI, 2016). Since both the Manipur River basin and Dhansiri River basin are closer in spatial proximity (Figure 7), they may have physically similar characteristics (Table 3); therefore, the observed river discharge of the Dhansiri River was used to calibrate the hydrological model for Manipur River basin. Rather than directly using the observed discharge of Dhansiri River, the area-ratio method was applied to the dataset. Rainfall data of Imphal and Dimapur rain gauge stations which lie in the center of Manipur River and Dhansiri River basins were compared. Imphal receives an average annual rainfall of 1350–1400 mm, and Dimapur receives an average annual rainfall of 1450–1500 mm. Since the average annual rainfall difference is around 5%, the rainfall compensating factor was ignored. A constant value of 0.59 obtained through area-ratio was multiplied to the observed discharge dataset as an area-ratio compensating factor.

The model was calibrated between the time periods 2007–2011 and validated between the 2012 and 2014 on monthly time steps, whereas the model was provided with a one-year warm-up period. Initially, the same sensitive parameters with the same ranges were selected, which were used for the calibration using the rating curve method. In addition to that, as a routing parameter the Manning value for the main channel (CH_N2) was added. From the sensitivity

TABLE 3 Properties of the recipient and donor basins.

Factor	Recipient	Donor
Precipitation (mm)	1350–1400	1450–1500
Dominant LULC	Wetland, forest, agriculture	Wetland, forest, agriculture
Elevation (m)	694–2642	81–3006
Annual average temperature (°C)	12–31	18–25
Slope (degree)	0–66	0–78
Area (km^2)	5020	8515
Soil	Haplohumults, dystrocrepts, hapludalfs, haplaquepts	Dystrochrepts, haplumbrepts, entrocrepts, udorthents

analysis the initial SCS runoff curve number for moisture condition II (CN2), the Manning value for the main channel (CH_N2), and the soil water capacity of the first soil layer (SOL_AWC) were found to be the most sensitive parameters. The significance of these parameters has been accounted for by other researchers. The flow parameters such as CH-N2 and CN2 play a significant role in the SWAT model calibration in areas which experience tropical to temperate type of climates (Emam et al., 2017; Vilaysane et al., 2015). Sensitive parameters are enlisted in Table 4. The model returned $R^2 = 0.46$, KGE = 0.64 and $R^2 = 0.40$, KGE = 0.63 during calibration and validation respectively. Scatter plots for calibration and validation are shown in Figure 8. From the model performance statistics, the two discharges show slightly low coefficient of determination, but still the statistical measure KGE shows better performance. This may happen as the concurrent overestimation and underestimate of discharge might raise the KGE score. These compensating flaws could favour bias and variability factors, maintaining the performance criteria's overall high score. This may result in a higher criterion score overall without raising the model's relevance.

3.4 | Calibration based on water level and river bathymetry

The model was calibrated between the time periods 2009–2015 and validated between 2016 and 2018 on a monthly time scale, whereas the year 2008 was used as a warm-up period for the model. Similar to the previous approach, the sensitive parameters used in the rating curve-based calibration approach were imported with the same ranges. In order to obtain the best fit, several iterations were carried out by changing the ranges of the variables and by combining the other routing parameters. An extra routing parameter was added in the calibration and validation in terms of the Manning's value for the main channel (CH_N2). The most sensitive parameters, along with the fitting values, are shown in Table 4. SOL-AWC, HRU-SLP and

TABLE 4 SWAT parameters with their fitting value and level of sensitivity for four different calibration approaches.

S. No.	Parameters	Description	Calibration based on rating curve		Calibration based on SSEBop actual evapotranspiration		Calibration based on regionalization (physical similarity)		Calibration based on river bathymetry	
			Fitted value	Sensitivity	Fitted value	Sensitivity	Fitted value	Sensitivity	Fitted value	Sensitivity
1	CN2 Initial SCS	Initial SCS runoff curve number for moisture condition II	−21.87	High	−43.25	High	1	High	−19.5	Medium
2	ALPHA_BF Baseflow	Baseflow alpha factor	0.99	High	0.96	Low	0.99	Medium	0.99	High
3	GW_DELAY Groundwater	Groundwater delay	−3.25	Medium	−7.75	Medium	14.75	Low	−12.5	Low
4	HRU_SLP Average	Average slope steepness	0.61	Low	0.68	Low	0.57	Medium	0.68	High
5	ESCO Soil	Soil evaporation compensation factor	0.2	Medium	0.59	High	0.3	Medium	0.65	Medium
6	SOL_AWC Soil water	Soil water capacity of the first soil layer	6.98	High	24.8	Medium	1.04	High	5.62	High
7	CH_N2 Manning	Manning value for main channel	–	–	–	–	30.62	Medium	36.12	Low
8	EPCO	Plant uptake compensation factor	–	–	0.57	High	–	–	–	–
9	CAN_MX	Maximum canopy storage	–	–	0.64	High	–	–	–	–

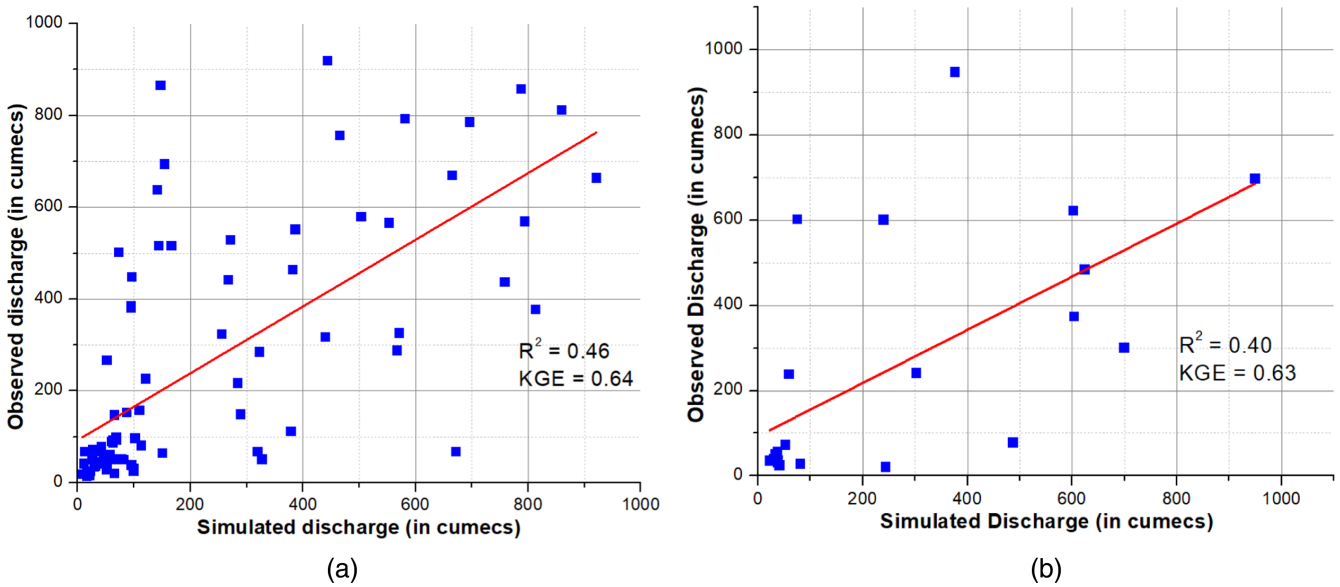

FIGURE 8 (a) Calibration. (b) Validation of model based on regionalization approach.

ALPHA_BF were found to be the most sensitive variables among all. During the calibration and validation period the model returned a good degree of agreement with $R^2 = 0.79$, KGE = 0.83 and $R^2 = 0.62$, KGE = 0.77 respectively. It can also be noted that the model performance was found to be better during calibration than validation because there was a higher uncertainty involved in the year

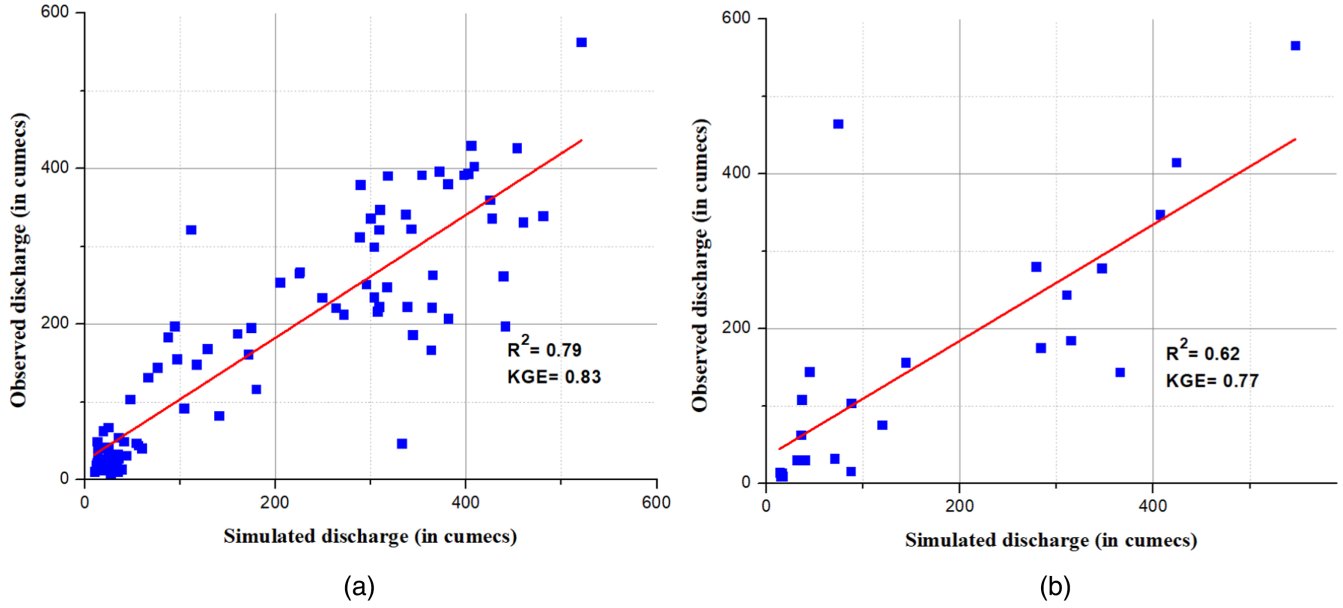

FIGURE 9 (a) Calibration. (b) Validation of model based on water level and river bathymetry approach.

2017 due to the higher amount of precipitation. The model performance statistics indicate better agreement during the calibration period than the validation period. The scatter plot indicating the degree of agreement for calibration and validation is shown in Figure 9. Though the P-factor value was found to be low with its value ranging around 0.55, the R-factor statistics associated with the model indicate a lower degree of uncertainty.

4 | DISCUSSION

The calibration of hydrological models is subjective in nature and the knowledge of the expert in relation to calibration problems and basin hydrology cannot be replaced by any automatic algorithm related to calibration. Findings of this study shows that among the four different calibration approaches, model performance was very good for calibration based on (i) stage-discharge curve using spatial proximity approach and (ii) water level and river bathymetry, good for calibration based on the SSEBop actual evapotranspiration, and satisfactory for calibration based on the river discharge using the physical similarity regionalization approach. During calibration, the coefficient of determination (R^2) and the Kling Gupta Efficiency (KGE) were found to be in the range of 0.46–0.81 and 0.41–0.83 respectively, whereas during validation R^2 and KGE were found to be in the range of 0.40–0.79 and 0.53–0.77 for all the four different techniques. Among the four calibration techniques used, three were based on streamflow, whereas the one was based on evapotranspiration, both are the components of water balance. Initial SCS runoff curve number for the moisture condition-II was the most sensitive parameter in both calibrations based on streamflow and evapotranspiration. When the model was calibrated based on streamflow datasets, baseflow alpha factor and soil water capacity of first soil layer were found to be the most sensitive parameters. Soil evaporation compensation factor, plant uptake compensation factor and maximum canopy coverage were found to be more sensitive when the calibration was done using evapotranspiration datasets. Several restrictions were encountered in this study in obtaining the satisfactory result. Due to inadequate rainfall-runoff data and gauging locations, multiple sites calibration of the model at sub-basin scale was not possible. The use of high-resolution DEM using stereo-pair satellite imagery could have increased the accuracy of streamflow estimation of the SWAT model both in terms of its spatial and temporal variability.

The calibration using rating curve based on spatial proximity approach fetched a very good result in terms of model performance. Though the model performance was good, however, during the high flow season the model performance was found to be unsatisfactory as it was unable to match the observed peak flow. The poor performance on the SWAT model in capturing the high streamflow fluxes may be associated with three major reasons. Firstly, the lower accuracy and higher uncertainty of generated rating curve in the wet season with comparatively lower coefficient of determination as compared to the dry season. Secondly, the poor depiction of high streamflow fluxes can be uncertainty associated with the rainfall measurement and filling the missing data using weather generator tool. Thirdly, it may be attributed to weakness of regionalization approach using spatial proximity, since the rating curve used in this study to compute the streamflow at the outlet using stage data was located six kilometres upstream of the outlet point. A similar kind of trend was observed by Odusanya et al. (2022) while calibrating the hydrological model for ungauged Ogun River Basin using the streamflow of Oueme River Basin. However, an attempt was made to eliminate the drawback due to spatial proximity by introducing a new approach with the integration of remote sensing datasets with river bathymetry obtained from echo-sounder. The discharge was derived integrating remote sensing

datasets (Kebede et al., 2020; Sichangi et al., 2018; Xiong et al., 2021) and river bathymetry. The results obtained from this new integrated approach produced slightly better result with higher Kling-Gupta efficiency, p-factor and lower r-factor.

The calibration based on physical similarity of the basin fetched inferior result when it was compared with the other three approaches applied in this study. The main reasons behind the higher uncertainty and under performance of the model can be the slightly higher amount of rainfall in the Dhansiri River basin, steep topography in the Dhansiri River basin as compared to the Manipur River basin, the minor variation in the geometry of the main channel, and Manning's roughness at the outlet point. Secondly, it can be due to uneven distribution of rainfall especially in the southern part of Dhansiri River which receives comparatively higher amount of rainfall. For determining the physical similarity between the Manipur River basin and Dhansiri River basin, only the meteorological estimates of Imphal and Dimapur weather stations (both the basins lie in the valley regions of the respective basins) were compared. But the upper reaches of the Dhansiri River basin receive higher amount of rainfall compared to the lower valley reaches. But no comparison was done with rainfall received in the upper reaches of the Dhansiri River basin as this area does not have any ground weather station. One of the main reasons behind the absence of weather gauge station in the upper reaches is the area is dominated by dense forest and they are mostly inhabitant. These uncertainties in the rainfall estimations may have led to poor model performance of the model during calibration with streamflow of Dhansiri River based physical similarity approach. Similar kind of drawbacks has been observed while using the physical similarity-based regionalization approach for Oueme River basin and Ghareshoo area of Iran (Mosavi et al., 2021; Odusanya et al., 2022).

The calibration based on SSEBop datasets derived from MODIS fetched better result as compared to calibration using streamflow data based on physical similarity. Values of both SSEBop evapotranspiration and evapotranspiration simulated varied as per seasonal variability, but the evapotranspiration simulated from SWAT was having higher variability as compared to that of SSEBop evapotranspiration derived from MODIS. The main reason could be the SWAT considers actual land surface conditions (slope, soil and LULC) and climate data (wind speed, temperature and relative humidity) for the estimation of evapotranspiration estimation, whereas the SSEBop evapotranspiration derived from MODIS is solely based on vegetation and climate remote sensing data (leaf area index, enhanced vegetation index, land surface temperature and fraction of photosynthetically active radiation) (Khan et al., 2018; Parajuli et al., 2022). The computation of evapotranspiration is highly dependent on the growth of the crop, but it is infeasible to compute the crop growth on a monthly time scale. Since the SSEBop evapotranspiration derived from MODIS was on the higher side as compared to that of evapotranspiration simulated by SWAT during dry season led higher estimation on annual basis by SSEBop product. The evapotranspiration simulated by SWAT was higher during the growing season of crop but lesser during the cold and dry seasons, whereas SSEBop evapotranspiration derived from MODIS did not vary as per the cropping seasons. It can be observed that evapotranspiration simulated are more accurate than that of SSEBop evapotranspiration product as it can represent variability as per cropping patterns (Parajuli et al., 2022). The major limitation of this study is the availability of long time series data. The hydrological model calibration and validation was carried on monthly temporal scale, however there is scope of study which can carried out daily temporal scale streamflow datasets. The multi-site calibration and validation was not feasible due to the lack of observed stage and streamflow data at sub-basin scale.

5 | CONCLUSIONS

For the evaluation of performance of calibration of hydrological model using various approaches, the SWAT hydrological model was setup in the data scarce Manipur River basin. Multiple calibration techniques were applied based on a stage-discharge curve using spatial proximity approach, MODIS (MOD 16) actual evapotranspiration, river discharge using a physical similarity regionalization approach, water level, and river bathymetry. Among the four techniques applied in this study, calibration based on (i) stage-discharge curve using spatial proximity approach and (ii) water level and river bathymetry was found to be a better approach as compared to (iii) SSEBop actual evapotranspiration and (iv) river discharge using physical similarity regionalization approach in Manipur River basin as indicated by the statistical indices. The degree of agreement was low due to the level of uncertainty in the SSEBop AET, probably because of the uncertainty associated with the climate and retrieving algorithm. In the case of river discharge using the physical similarity technique, the lower degree of agreement can be probably because of the geometric profile of the main stream at the outlet and variation in topography of the donor basin. The findings of this study clearly indicate that the hybrid approach by integrating remote sensing datasets along with field measured river bathymetry data to estimate the river discharge to calibrate the SWAT model can be used for the streams with narrow width where remote sensing datasets have limitations due to its spatial resolution. In this study, regionalization based on physical similarity was applied. However, there is further scope to apply regionalization approaches to transfer the sensitive parameters from the donor basin to the target basin. In the case of the ET based calibration approach, this study discusses only the SWAT model run on Penman-Monteith and SSEBop evapotranspiration product; there is the future scope of a study which can be done based on other algorithms such as Priestly-Taylor and Hargreaves and other available datasets such as GLEAM. The findings of this study suggest that the SWAT model can be efficiently calibrated using (i) stage-discharge curve based on spatial proximity approach, and (ii) water level and river bathymetry can be used as a potential decision support tool for the advanced studies on basin hydrology, eco-hydrology and eco-hydraulic in an ungauged basin.

ACKNOWLEDGEMENTS

The authors express their heartfelt gratitude to the United States Geological Survey, Alaska Satellite Facility, Directorate of

Environment, Govt. of Manipur, National Bureau of Soil Survey & Land Use Planning, Govt. of India, Loktak Development Authority, NHPC Loktak Project, Inland Waterways Authority of India and National Remote Sensing Centre, Govt. of India for providing the valuable database. We would like to thank Mukesh Kumar Yadav, Laishram Kishan Singh, Pukhrambam Kesomani Singh, Kh Digbijoy Singh and Rajkumari Neetu Sana for supporting us during the extensive field campaigns. Last but not the least, we thank the editor Prof. Doerthe Tetzlaff and reviewers for very constructive and helpful suggestions. The research outcome of this study was supported by SERB sponsored project (CRG/2021/006665) and the National Institute of Technology Manipur. The first author would like thank the Ministry of Education, Govt. of India, and the Deutscher Akademischer Austauschdienst for providing the prestigious DAAD Doctoral Fellowship to carry out this study. Open Access funding enabled and organized by Projekt DEAL.

CONFLICT OF INTEREST STATEMENT

The authors declare no conflict of interest exists.

DATA AVAILABILITY STATEMENT

The data that support the findings of this study are available on request from the corresponding author. The data are not publicly available due to privacy or ethical restrictions.

ORCID

Vicky Anand https://orcid.org/0000-0001-7087-1344

REFERENCES

Abbaspour, K. C. (2015). *SWAT-CUP: SWAT calibration and uncertainty programs–A user manual* (p. 100). Swiss Federal Institute of Aquatic Science and Technology.

Abbaspour, K. C., Johnson, C. A., & van Genuchten, M. T. (2004). Estimating uncertain flow and transport parameters using a sequential uncertainty fitting procedure. *Vadose Zone Journal*, *3*, 1340–1352. https://doi.org/10.2136/vzj2004.1340

Ajami, N. K., Gupta, H., Wagener, T., & Sorooshian, S. (2004). Calibration of a semi-distributed hydrologic model for streamflow estimation along a river system. *Journal of Hydrology*, *298*, 112–135.

Ali, M. H., Popescu, I., Jonoski, A., & Solomatine, D. P. (2023). Remote sensed and/or global datasets for distributed hydrological modelling: A review. *Remote Sensing*, *15*, 1642. https://doi.org/10.3390/rs15061642

Anand, V., Oinam, B., & Parida, B. R. (2020). Uncertainty in hydrological analysis using multi-GCM predictions and multi-parameters under RCP 2.6 and 8.5 scenarios in Manipur River basin, India. *Journal of Earth System Science*, *129*, 223. https://doi.org/10.1007/s12040-020-01492-z

Anand, V., Oinam, B., & Wieprecht, S. (2023). Assessment and comparison of DEM generated using Cartosat-1 stereo pair data for hydrological applications. *Journal of the Indian Society of Remote Sensing.*, *51*, 483–496. https://doi.org/10.1007/s12524-022-01639-z

Arnold, J. G., & Fohrer, N. (2005). SWAT-2000: Current capabilities and research opportunities in applied watershed modeling. *Hydrological Processes*, *19*(3), 563–572.

Arnold, J. G., Srinivasan, R., Muttiah, R. S., & Williams, J. R. (1998). Large area hydrologic modeling and assessment part I: Model development, JAWRA. *Journal of the American Water Resources Association*, *34*(73–89), 1998. https://doi.org/10.1111/j.17521688.1998.tb05961.x

Babel, L., & Karssenberg, D. (2013). Hydrological models are mediating models. *Hydrology and Earth System Sciences*, *10*(8), 10535–10563.

Bardossy, A. (2007). Calibration of hydrological model parameters for ungauged basins. *Hydrology and Earth System Sciences*, *11*(2), 703–710.

Bastola, S., Ishidaira, H., & Takeuchi, K. (2008). Regionalisation of hydrological model parameters under parameter uncertainty: A case study involving TOPMODEL and basins across the globe. *Journal of Hydrology*, *357*, 188–206. https://doi.org/10.1016/j.jhydrol.2008.05.007

Bennour, A., Li, J., Massimo, M., Chaolei, Z., Yelong, Z., Beatrice, A. B., & Min, J. (2022). Calibration and validation of Swat model by using hydrological remote sensing observables in the Lake Chad Basin. *Remote Sensing*, *14*(6), 1511. https://doi.org/10.3390/rs14061511

Bicknell, B. R., Imhoff, J. C., Kittle, J. L., Jr., Donigian, A. S., Jr., & Johanson, R. C. (1997). *Hydrological simulation program-Fortran, User's manual for version 11* (p. 755). U.S. Environmental Protection Agency, National Exposure Research Laboratory.

Bureau, R. (2016). *The list of wetlands of international importance;Ramsar secretariat* (pp. 1–48). Ramsar Convention Secretariat.

Chen, M., Senay, G. B., Singh, R. K., & Verdin, J. P. (2016). Uncertainty analysis of the Operational Simplified Surface Energy Balance (SSEBop) model at multiple flux tower sites. *Journal of Hydrology*, *536*, 384–399. https://doi.org/10.1016/j.jhydrol.2016.02.026

Chow, V. T. (1959). *Open channel hydraulics*. McGraw-Hill.

Coon, W. F. (1998). *Estimation of roughness coefficients for natural stream channels with vegetated Banks*. US Geological Survey.

Cunge, J. A. (1969). On the subject of a flood propagation computation method (Muskingum method). *Journal of Hydraulic Research*, *7*(2), 205–230.

Directorate of Environment. (2013). Government of Manipur.

Dudley, S. J., Bonham, C. D., Abt, S. R., & Fischenich, J. C. (1998). Comparison of methods for measuring Woody riparian vegetation density. *Journal of Arid Environments*, *38*(1), 77–86. https://doi.org/10.1006/jare.1997.0314

Emam, A. R., Kappas, M., Linh, N. H. K., & Renchin, T. (2017). Hydrological modeling and runoff mitigation in an ungauged basin of central Vietnam using SWAT model. *Hydrology*, *4*(1), 16. https://doi.org/10.3390/hydrology4010016

Ewen, J., Parkin, G., & O'Conell, P. E. (2000). SHETRAN: Distributed River Basin flow modeling system. *Journal of Hydrologic Engineering*, *5*, 250–258.

Getirana, A. C. V. (2010). Integrating spatial altimetry data into the automatic calibration of hydrological models. *Journal of Hydrology*, *387*, 244–255.

Gupta, H. V., Kling, H., Yilmaz, K. K., & Martinez, G. F. (2009). Decomposition of the mean squared error and NSE performance criteria: Implications for improving hydrological modeling. *Journal of Hydrology*, *377*, 80–91.

Huang, Q., Long, D., Du, M., Han, Z., & Han, P. (2020). Daily Continuous River discharge estimation for ungauged basins using a hydrologic model calibrated by satellite altimetry: Implications for the SWOT Mission. *Water Resources Research*, *56*, e2020WR027309.

Immerzeel, W. W., & Droogers, P. (2008). Calibration of a distributed hydrological model based on satellite evapotranspiration. *Journal of Hydrology*, *349*, 411–424.

Inland Waterways Authority of India (IWAI). (2016). Preparation of two stage detailed project report (DPR) of proposed cluster 2 inland waterways feasibility report for NW-31 Dhansiri/Chathe River. http://iwai.nic.in/sites/default/files/5863383100NW-31%20Dhansiri%20Final%20FSR.pdf

Kebede, M. G., Lei, W., Kun, Y., Deliang, C., Xiuping, L., Tian, Z., & Zhidan, H. (2020). Discharge estimates for ungauged Rivers flowing

over complex high-mountainous regions based solely on remote sensing-derived datasets. *Remote Sensing*, *12*(7), 1064.

Khan, M. S., Liaqat, U. W., Baik, J., & Choi, M. (2018). Stand-alone uncertainty characterization of GLEAM, GLDAS and MOD16 evapotranspiration products using an extended triple collocation approach. *Agricultural and Forest Meteorology*, *252*, 256–268.

LDA. (2003). *Extension proposal. Sustainable development and water resource management of Loktak Lake*. Loktak Development Authority and Wetlands International South Asia.

Liang, X., Lettenmaier, D. P., Wood, E. F., & Burges, S. J. (1994). A simple hydrologically based model of land surface water and energy fluxes for general circulation models. *Journal of Geophysical Research*, *99*, 14415–14428. https://doi.org/10.1029/94JD00483

Liu, G., Schwartz, F. W., Tseng, K.-H., & Shum, C. K. (2015). Discharge and water-depth estimates for ungauged rivers: Combining hydrologic, hydraulic, and inverse modeling with stage and water-area measurements from satellites. *Water Resources Research*, *51*, 6017–6035. https://doi.org/10.1002/2015WR016971

Lou, H., Zhang, Y., Yang, S., Wang, X., Pan, Z., & Luo, Y. (2022). A new method for long-term river discharge estimation of small- and medium-scale Rivers by using multisource remote sensing and RSHS: Application and validation. *Remote Sensing.*, *2022*(14), 1798. https://doi.org/10.3390/rs14081798

Manning, R. (1891). On the flow of water in open channels and pipes. *Transactions of the Institution of Civil Engineers of Ireland*, *20*, 161–207.

Mengistu, A. G., Leon, D., & van Rensburg, Y. (2019). Techniques for calibration and validation of SWAT model in data scarce arid and semi-arid basins in South Africa. *Journal of Hydrology: Regional Studies*, *25*, 100621. https://doi.org/10.1016/j.ejrh.2019.100621

Mosavi, A., Golshan, M., Choubin, B., Ziegler, A. D., Sigaroodi, S. K., Zhang, F., & Dineva, A. A. (2021). Fuzzy clustering and distributed model for streamflow estimation in ungauged watersheds. *Scientific Reports*, *11*, 8243.

National Bureau of Soil Survey and Land Use Planning. (2001). *Land capability classes of basin area of Loktak Lake*. NBSS and LUP.

Neitsch, S. L., Arnold, J. G., Kiniry, J. R., & Williams, J. R. (2011). *Soil and water assessment tool theoretical documentation version 2009*. Texas Water Resources Institute.

Neitsch, S. L., Arnold, J. G., Kiniry, T., Srinivasan, R., & Williams, J. R. (2002). *Soil and water assessment tool User's manual version 2002*. Texas Water Resources Institute.

Odusanya, A. E., Karsten, S., & Bano, M. (2022). Using a regionalisation approach to evaluate streamflow simulated by an Ecohydrological model calibrated with global land surface evaporation from remote sensing. *Hydrology and Earth System Sciences*, *40*, 101042. https://doi.org/10.1016/j.ejrh.2022.101042

Odusanya, A. E., Mehdi, B., Schürz, C., Oke, A. O., Awokola, O. S., Awomeso, J. A., Adejuwon, J. O., & Schulz, K. (2019). Multi-site calibration and validation of SWAT with satellite-based evapotranspiration in a data-sparse catchment in southwestern Nigeria. *Hydrology and Earth System Sciences*, *23*, 1113–1144. https://doi.org/10.5194/hess-23-1113-2019,2019

Parajuli, P. B., Avay, R., Ying, O., & Anita, T. (2022). Comparison of SWAT and MODIS evapotranspiration data for multiple timescales. *Hydrology*, *9*(6), 103.

Paris, A., Dias de Paiva, R., Santos da Silva, J., Medeiros Moreira, D., Calmant, S., Garambois, P.-A., Collischonn, W., Bonnet, M.-P., & Seyler, F. (2016). Stage-discharge rating curves based on satellite altimetry and modeled discharge in the Amazon Basin. *Water Resources Research*, *52*, 3787–3814.

Pechlivanidis, I., Jackson, B., McIntyre, N., & Wheater, H. (2011). Basin scale hydrological modelling: A review of model types, calibration approaches and uncertainty analysis methods in the context of recent developments in technology and applications. *Global NEST Journal*, *13*(3), 193–214.

Petković, D., Gocic, M., Trajkovic, S., Shamshirband, S., Motamedi, S., Hashim, R., & Bonakdari, H. (2015). Determination of the most influential weather parameters on reference evapotranspiration by adaptive neuro-fuzzy methodology. *Computers and Electronics in Agriculture*, *114*, 277–284.

Qi, J., Zhang, X., Yang, Q., Srinivasan, R., Arnold, J. G., Li, J., Waldholf, S. T., & Cole, J. (2020). SWAT ungauged: Water quality modeling in the upper Mississippi river basin. *Journal of Hydrology*, *584*, 124601. https://doi.org/10.1016/j.jhydrol.2020.124601

Senay, G. B., Bohms, S., Singh, R. K., Gowda, P. H., Velpuri, N. M., Alemu, H., & Verdin, J. P. (2013). Operational evapotranspiration mapping using remote sensing and weather datasets: A new parameterization for the SSEB approach. *Journal of the American Water Resources Association*, *49*(3), 577–591.

Sichangi, A., Wang, L., & Hu, Z. (2018). Estimation of river discharge solely from remote-sensing derived data: An initial study over the Yangtze river. *Remote Sense*, *10*, 1385. https://doi.org/10.3390/rs10091385

Sichangi, A. W., Wang, L., Yang, K., Chen, D., Wang, Z., Li, X., Zhou, J., Liu, W., & Kuria, D. (2016). Estimating Continental River basin discharges using multiple remote sensing data sets. *Remote Sensing of Environment*, *179*, 36–53.

Singh, C. R., Thompson, J. R., French, J. R., Kingston, D. G., & Mackay, A. W. (2010). Modeling the impact of prescribed global warming on the runoff from headwater basins of the Irrawaddy River and their implications for the water level regime of Loktak Lake, Northeast India. *Hydrology and Earth System Sciences*, *14*, 1745–1765.

Singh, C. R., Thompson, J. R., Kingston, D. G., & French, J. R. (2011). Modelling water-level options for ecosystem services and assessment of climate change: Loktak Lake, Northeast India. *Hydrological Sciences Journal*, *56*(8), 1518–1542.

Singh, S. K., Augas, J., Pahlow, M., & Graham, S. (2020). Methods for regional calibration-a case study using the Topnet hydrological model for the bay of plenty region, New Zealand. *The Australasian Journal of Water Resources*, *24*(2), 153–166.

Singh, S. K., & Bárdossy, A. (2015). Hydrological model calibration by sequential replacement of weak parameter sets using depth function. *Hydrology*, *2*, 69–92.

Sirisena, T. A. J. G., Maskey, S., & Ranasinghe, R. (2020). Hydrological model calibration with streamflow and remote sensing based evapotranspiration data in a data Poor Basin. *Remote Sensing*, *12*, 3768. https://doi.org/10.3390/rs12223768

Sokolowski, J., & Banks, C. (2010). *Modeling and simulation fundamentals: Theoretical underpinnings and practical domains*. John Wiley and Sons.

Sun, W., Ishidaira, H., & Bastola, S. (2012). Calibration of hydrological models in ungauged basins based on satellite radar altimetry observations of river water level. *Hydrological Processes*, *26*, 3524–3537.

Swain, J. B., & Patra, K. C. (2017). Streamflow estimation in ungauged catchments using regionalization techniques. *Journal of Hydrology*, *554*, 420–433.

Tarpanelli, A., Barbetta, S., Brocca, L., & Moramarco, T. (2013). River discharge estimation by using altimetry data and simplified flood routing modeling. *Remote Sense*, *5*, 4145–4163.

Tessema, S. (2011). *Hydrological modeling as a tool for sustainable water resources management: A case study of the Awash River basin (doctoral dissertation)*. KTH Royal Institute of Technology.

Thomas, C., Diekkrüger, B., & Giertz, S. (2013). A comparison of hydrological models for assessing the impact of land use and climate change on discharge in a tropical basin. *Journal of Hydrology*, *498*, 221–236.

Vilaysane, B., Takara, K., Luo, P., Akkharath, I., & Duan, W. (2015). Hydrological stream flow modelling for calibration and uncertainty analysis using SWAT model in the Xedone River basin, Lao PDR. *Procedia Environmental Sciences*, *28*, 380–390.

Wu, H., & Chen, B. (2015). Evaluating uncertainty estimates in distributed hydrological modeling for the Wenjing River watershed in China by GLUE, SUFI-2, and ParaSol methods. *Ecological Engineering*, *76*, 110–121.

Xiong, J., Shenglian, G., & Jiabo, Y. (2021). Discharge estimation using integrated satellite data and hybrid model in the midstream Yangtze River. *Remote Sense*, *13*(12), 2272. https://doi.org/10.3390/rs13122272

Xueying, L., Di, L., Louise, J., Simon, M., Muhammad, S., Pengfei, H., & Fanyu, Z. (2023). Soil moisture to runoff (SM2R): A data-driven model for runoff estimation across poorly gauged Asian water towers based on soil moisture dynamics. *Water Resources Research*, *59*, 3. https://doi.org/10.1029/2022WR033597

How to cite this article: Anand, V., Oinam, B., Wieprecht, S., Singh, S. K., & Srinivasan, R. (2024). Enhancing hydrological model calibration through hybrid strategies in data-scarce regions. *Hydrological Processes*, *38*(2), e15084. https://doi.org/10.1002/hyp.15084